DESIGN PROCEDURE FOR A DISSIPATIVE ANCHORING SYSTEM FOR THE SEISMIC UPGRADE OF HISTORIC BUILDINGS

V. Melatti [(1)], D. D'Ayala [(2)]

[(1)] *PhD student, University College London, victor.melatti.16@ucl.ac.*
[(2)]*Professor, University College London, .d.dayala@ucl.ac.uk*

Abstract

Masonry structures represent the largest portion of the building stock in regions affected by destructive earthquakes and show high vulnerability to seismic sequences. In particular, poor-quality connections between adjacent resisting elements often determines the outward detachment of the walls causing the local/global collapse of the building. In the last decades, a number of technical solutions have been developed to prevent such mechanism, and current design codes, both in the case of newly built and of heritage structures, acknowledge the importance of effective structural connections. For instance, cross-ties have been widely implemented to connect the perimeter walls of masonry structures in many historic city centres across Europe, proving to be an effective tool to restore the box-like behaviour and distribute the seismic forces through all the resisting elements. Nonetheless, the installation of steel ties into historical buildings increases the local stiffness at the corner's location, leading to high-stress concentration in case of seismic events and consequently to severe damage to the valuable parent material in which the cross-ties are embedded. To tackle these issues, an innovative friction-based dissipative device connected in series with stainless steel anchors is presented. The assembly is designed to be inserted at the connection between perpendicular walls: the stainless steel profiles improve the box-like behaviour of the building, while the device allows a controlled displacement between orthogonal sets of walls, which determines the energy dissipation capacity of the strengthened connection. In this paper, the nonlinear equilibrium equation of a monolithic wall restrained by the dissipative anchoring system is presented. By computing the collapse load factor for a set of rotated configurations around a hinge point, the capacity curve for the restrained system is obtained. The dissipative device provides additional ductility capacity to the system, and the stability of the restrained wall is checked within the framework of the performance-based design. Following the N2 method, the capacity curve is compared with the inelastic demand spectra to determine the performance point at which the inelastic demand crosses the capacity curve. The obtained performance point is compared with those obtained for a wall restrained by a traditional cross-tie under the same seismic action. The results show that the implementation of the dissipative device increments the ductility capacity of the system by 43% with comparison to a wall restrained by a traditional tie-rod. This results allows for a further reduction in the seismic demand and increases the displacement that determines the ultimate collapse. The performance point is found within the system capacity only for the case of the dissipative system, while the initial design of the traditional tie was found not adequate to sustain the seismic demand. By increasing its diameter, the tie is able to sustain the seismic force, but it would require a most invasive intervention that could hinder the original aesthetic of the building.

Keywords: Historical buildings, dissipative system, tie bar, friction device

1. Introduction

Damage to monumental masonry buildings caused by seismic events [1], [2], [3] highlights that their load bearing elements often separate into macroelements [4], which in turn are characterized by a mostly independent structural behaviour with respect to the rest of the building[5], [6]. Churches, for instance, often experience local failure due to the low tensile strength of the masonry, their intrinsic architectonic complexity (presence of bell-towers, vaults) and vulnerability (wide halls, large unrestrained façades, etc). Poor-quality connections between orthogonal structural walls greatly affect the dynamic performance of heritage masonry structures causing the relative detachment of masonry panels and ultimately the out-of-plane failure of the more vulnerable macroelements in the whole construction, while other portion of the building survive the shaking. A way of tackling this issue is to insert steel cross-ties at the corner of orthogonal walls in order to restore the box-like behaviour and restrain the out-of-plane movement of these weaker walls [7]. The tie can be designed according to a force-based procedure [8] to obtain the load multiplier that determines the collapse mechanism as a function of the peak ground acceleration (a_g), given a specific site, an intensity return period and an expected performance level of life safety:

$$\lambda_0 = \frac{a_g S F_c e^*}{q} \tag{1}$$

where S = site response coefficient, F_c = confidence factor, e^* = participating mass factor, q = behaviour factor. With reference to Figure 1c, the design force, F_t, is obtained by imposing the equilibrium between the system's forces:

$$F_t H_t = \lambda_0 mg \frac{H}{2} - \frac{mgB}{2} \tag{2}$$

where *H, B, m* are height, thickness and mass of the wall, respectively, and H_t is the height of installation of the tie in the wall, from the wall's constrained base. Hence:

$$F_t = mg \frac{\lambda_0 H - B}{2H_t} \tag{3}$$

Using this simple method, the number and dimensions of anchors per metre length of the wall, needed to prevent the wall from overturning due to the seismic action, can be determined. Nonetheless, for the case of monumental buildings, the increased local stiffness at the anchor's location might lead to high-stress concentration in case of seismic events and consequently to severe damage to the valuable parent material in which the cross-ties are embedded [7].

The seismic performance of the macroelements, prone to local damage and collapse mechanisms, can be evaluated also according to different methods within the framework of performance-based design [9]. By accounting for the postelastic displacement capacity of a restrained wall, it is possible to reduce the seismic demand by a factor R_μ and reduce the maximum forces that the ties would exert on the parent masonry [10]. To further improve the seismic response of a building, modern design codes recommend the use of devices able to provide ductility and energy dissipation in case of seismic action [11]. In this work, the performance-base design of a wall strengthened by an innovative friction-based anchoring system is presented. This system was proposed by D'Ayala and Paganoni to provide historic masonry structures with ductility and dissipation capacity [12]. The initial prototype of the dissipative device, patented in 2014 [13], was refined to achieve repeatable performance under cyclic load and ensure that the installation of the system has a minimal impact on the building in terms of loss of original material and aesthetic compatibility. The studies conducted from 2014 to the present day led to the revised prototype presented in this paper. Details on the device's properties and system's mechanism can be found in [14] and [15]. The results of the design are compared with those obtained for an unrestrained wall and for a wall restrained by a traditional tie rod.

2

2. Analytical model

2.1 One-sided rotation of unrestrained block

OPCM 3431/2005 [16], the Italian national seismic code, permits evaluating the expected seismic performance of a structure according to the modern design principles of the displacement-based method. Assuming a non linear single-degree-of-freedom (SDOF) system equivalent to the structure, the capacity curve is derived by performing a pushover analysis that leads to the evaluation of the building lateral load versus its characteristic lateral displacement (usually the peak displacement of the building roof). The capacity curve is then compared with the seismic demand adequately reduced in order to take into account the inelastic building behaviour. The expected structural response for the earthquake is described by the Acceleration-Displacement point (referred as performance point PP) obtained by the intersection of the seismic demand and the seismic capacity curves.

This procedure can be applied to masonry structures, by deriving the capacity curves for each failure modes. D'Ayala [17] identified a set of 12 possible modes of local failure and used a static kinematic approach to identify the collapse load multiplier (λ) that determines each collapse. The values λ are computed taking into account the geometry and materials of the selected building as obtained from site inspections and laboratory tests. The lowest value of λ identifies the mechanism that is more likely to happen for the selected building. Having converted the parameters of the selected mechanisms to those corresponding to an equivalent nonlinear SDOF system, they can be compared with the seismic demand curves, as previously described for the method described in the OPCM 3431, and performance points can be derived. Lagomarsino et al. [6], [18] developed a second procedure that evaluates the structural capacity of the local mechanism through the equilibrium limit analyses. This procedure considers each resulting block to be subjected to dead loads and to horizontal seismic action, proportional to the dead loads through a coefficient α, under the hypotheses of non-tensile strength and unlimited compressive strength of masonry. The equilibrium configuration is varied by an infinitesimal rotation of the block around the Rotation Point O' (obtained by intersecting the block's base and the direction of the reaction force, as shown in Fig. 2) and the coefficient λ that induces the loss of equilibrium is obtained by the principle of virtual works for each configuration.

Focusing to the specific case of the one sided out-of-plane rocking motion of monumental buildings' walls, the equilibrium equation can be written as:

$$mg \, \mathrm{Rsin}(\alpha - \theta) - mg \, u_\theta(\vartheta) = \lambda \, mgR \cos(\alpha - \theta) \qquad (4)$$

With reference to Fig.1a, R is the distance between the centroid G and the geometrical corner O, g is the gravity acceleration, m is the mass of the wall, θ is the wall angular displacement, α is the arctan (B/H).
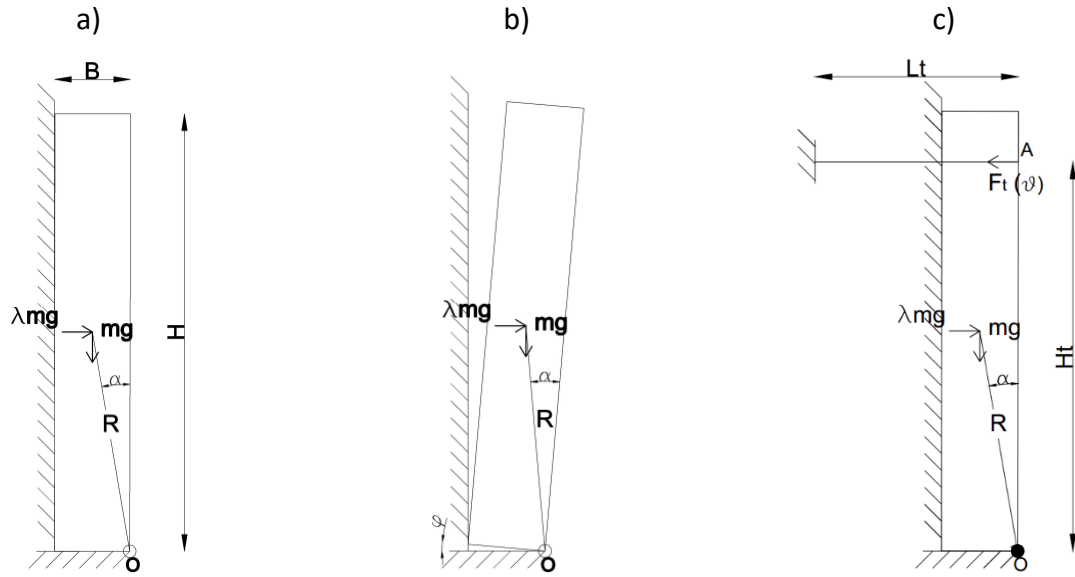
3

3d-0003

Fig. 1 - Geometrical parameters of one-sided rotation of a free wall in its a) resting position b) one-sided displaced configuration c) a wall restrained by a tie-rod.

To include the initial elastic stiffness and the compressive strength of the block f_m, a flexible interface can be modelled at the base of the block, as proposed by [19, [20, [21]. The interface has normal stiffness

$k_n = E/e$ (E = Young's modulus, e = thickness of the interface), and length L_h coincident with the wall length. During the rotation ϑ, $u_\theta(\vartheta)$, the distance between O and O', accounts for the change in position of the resultant reaction force as the rotation progress, while $mg\, u_\theta(\vartheta)$ represents the moment with respect to point O. Following Costa's approach [19], [20] and with reference to Fig. 2, the position of the reaction force is calculated for three different cases: (1) full contact, (2) partial contact with no crushing and (3) partial contact with crushing.

$$u_\theta(\vartheta) = \begin{cases} \dfrac{B}{2} - \dfrac{B^3 k_n L_h \theta}{12\, mg} & 0 < \theta \le \theta_{j0} \\[3mm] \dfrac{1}{3}\sqrt{\dfrac{2mg}{B^3 k_n L_h \theta}} & \theta_{j0} < \theta \le \theta_c \\[3mm] \dfrac{1}{2}\left(\dfrac{mg}{f_m L_h} + \dfrac{f_m^3 L_h}{12\, mg k_n^2 \vartheta^2}\right) & \theta \ge \theta_c \end{cases} \qquad (5)$$

The rotation identifying the crack limit is:

$$\theta_{j0} = \frac{2mg}{B^2 k_n L_h} \qquad (6)$$

While the critical rotation at which crushing begins, θ_c, namely for compressive stress equal to f_m is:

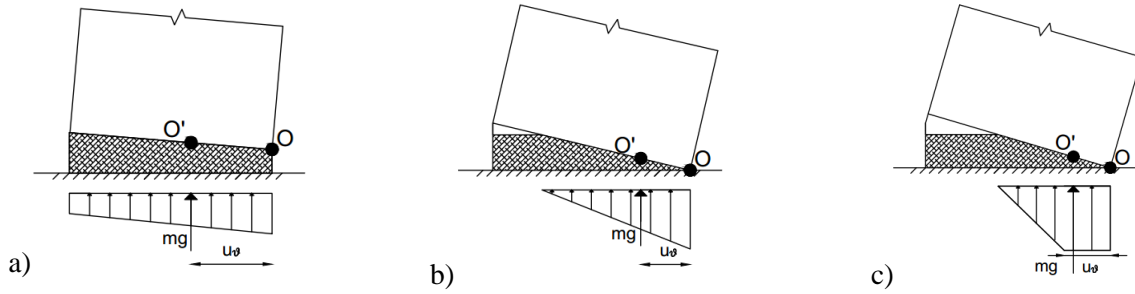$$\theta_c = \frac{f_m^2 L_h}{2 k_n mg} \qquad (7)$$

4

a)   b)   c)

Fig. 2. Evolution over rotation θ of interface stress distributions of a wall resting on a deformable interface of finite strength (a) full contact, (b) partial contact and (c) partial contact with crushing.

2.2 One-sided rotation of block restrained by anchor

The complexity of the model can be further increased by considering the restoring action provided by the introduction of a tie-rod, a typical intervention to improve the out-of-plane performance of perimeter walls [7]. The effectiveness of steel ties has been repeatedly confirmed by shake table tests [22], provided that masonry loss of integrity does not occur, and are usually designed to yield under severe ground motion accelerations. Concerning the tie force, it is considered horizontal throughout the analysis. The tie axial force is defined by the following parameters: F_t is the tie force at yield, H_t is the vertical distance between A and O (Fig. 1c), A is the cross-section area of tie, E is the Young modulus. The restoring moment provided by the tie can be written as:

$$F_t(\theta)H_t = \begin{cases} \dfrac{H_t \tan(\vartheta)}{L_t} EA\, H_t & 0 < \theta \le \theta_y \\ \epsilon_y EA\, H_t & \theta_y < \theta \le \theta_{pl} \\ 0 & \theta \ge \theta_{pl} \end{cases} \tag{8}$$

The rotation identifying the yielding of the anchor (θ_y) and the maximum deformation (θ_{pl}) are:

$$\theta_y = arctan(\epsilon_y\, L_t/H_t) \tag{9}$$

$$\theta_{pl} = arctan(\epsilon_{pl}\, L_t/H_t) \tag{10}$$

whit ϵ_y and ϵ_{pl} , the yielding and plastic strain of steel, taken as 0.2% and 1.6%, respectively. The equilibrium equation also considering the tie contribution is:

$$mg\,\text{R}\sin(\alpha - \theta) - mg\, u_\theta(\vartheta) + F_t(\theta)H_t = \lambda\, mgR\, \cos(\alpha - \theta) \tag{11}$$

Taking into account the contribution of the inward shift of the rotation point O' and the tie, the relationship between the overturning acceleration and the rotation can be derived, as shown in Fig. 3a. The values of the capacity curve are normalized with respect to those of a wall resting on a rigid interface, also shown in figure 3a.
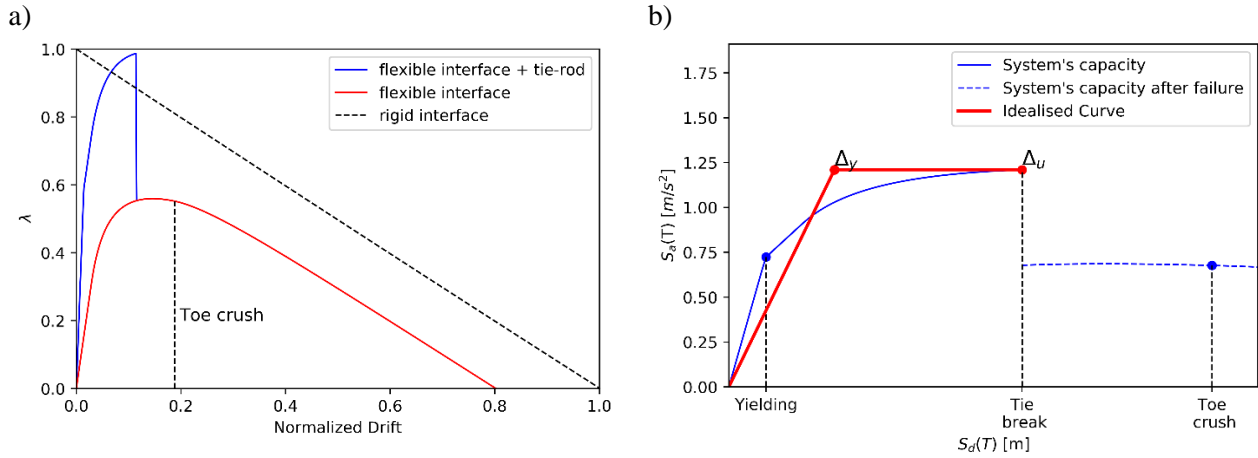
5

a)

b)

Fig. 3. a) Normalised capacity curve for rigid interface, flexible interface and flexible interface with tie; b) capacity curve of a wall restrained by a tie: real and idealised curve up to failure point.

From Fig. 3a it can be noted that the introduction of the flexible interface significantly reduces the capacity of the system with respect to a system overturning on a rigid interface. The use of anchors increases the initial stiffness of the systems and contributes to the stabilizing moment up to the failure of the steel element for $\theta = \theta_{pl}$. Figure 3b shows the capacity curve in terms of the displacement of a control point A corresponding to the front-end of the installed anchor (see Figure 1c): the first loss in the system's stiffness corresponds to the yielding of the bar, which behaves according to an elasto-plastic constitutive law up to its ultimate elongation. Given that the anchor is the first element to fail, the displacement corresponding to θ_{pl} is considered as the ultimate displacement for the system. After the bar's failure, the system experiences a sudden loss in strength capacity and the overturning moment is balanced by the self-weight of the wall only.

A linearized elasto-plastic relationship is adopted on the assumption that the linearized system will reach the same ultimate displacement Δu and acceleration S_{a_u} of the real system [11]. However, as it shows a plastic plateau, at an unknown displacement Δy the SDOF system yields and immediately reaches the maximum force that the system can resist. With reference to Fig.3b, by imposing that the areas (E) under the two curves are the same, the displacement Δy, can be computed:

$$\Delta_y = 2 \left(\Delta_u - \frac{S_{a_u}}{E} \right) \tag{12}$$

The elastic period of the linearized system can be deduced from the yielding acceleration and displacement that determine the last point of the elastic behaviour of the system:

$$T_{el} = 2\pi \sqrt{\frac{\Delta_y}{S_{a\,yield}}} \tag{13}$$

3. Performance-based design of traditional tie-rod

Within the framework highlighted in the previous section, the design of an anchor is performed by considering a target displacement of the system and compare it with the displacement demand of the seismic action. Regarding the derivation of the demand spectra, two broadly equivalent approaches exist: the N2 method [23] included in the EC8 and the capacity spectrum method with over-damped spectrum (CSM) [24]. The two methods differ essentially in the way the nonlinear demand spectrum is derived: the N2 method uses a reduction factor R as function of the structure expected ductility μ, while the CSM uses an equivalent-damping factor derived from the hysteresis loop of the structure. The N2 approach is the base of the evaluation of the seismic performance for this case study. The procedure requires the definition of the elastic and then of the

6

inelastic demand spectra in order to determine the performance point at which the inelastic demand intersect the idealised capacity curve. For the purpose of the analysis, an acceleration-displacement demand spectrum is required. The demand spectrum has been computed with respect to EC8 for the values reported in Table 2.

Table 2. Parameters for the computation of the elastic acceleration spectrum

S	Tb	Tc	Td	η	γ	ag
[-]	[s]	[s]	[s]	[-]	[-]	[g]
1.15	0.2	0.6	2	1	1.2	0.25

Code design of a tie-rod has been performed assuming steel S235 as specified in the Eurocode 3 [25]. Table 1 summarizes all the parameters for the assumed anchor.

Table 1 Assumed values for design of tie-rod

	0.2% Yield strength	1.6% Ultimate strength	L	Ht	φ (diameter)
	[MPa]	[MPa]	[m]	[m]	[m]
S235	235	235	4	4.5	0.03

The inelastic spectrum is obtained by reducing the elastic spectrum by the R_μ factor depending on the ductility capacity of the system:

$$R_\mu = \begin{cases} (\mu - 1)\dfrac{T_{el}}{T_c} + 1 & if \ T_{el} < T_c \\ \mu & if \ T_{el} > T_c \end{cases} \tag{14}$$

The ductility the restrained wall can provide is computed from the idealized curve:

$$\mu = \frac{\Delta_u}{\Delta_y} \tag{15}$$

Fig. 4a shows the inelastic spectrum obtained reducing the elastic A-D spectrum by a reduction factor corresponding to ductility of the system, μ, equal to 2.8. As the computed elastic period of the system is greater than the corner period of the spectrum, the assumption that the spectral displacement demand is equal to the intersect of the elastic branch of the capacity curve with the elastic spectrum is valid. From Fig. 4a it is clear that the ductility capacity provided by the anchor is not sufficient to provide the restrained system with the required demand in displacement. This result is also visible from a graphical point of view, given that the idealized capacity curve does not intersect the inelastic demand curve.

A way of improving the wall's capacity would be to increase the strength/stiffness of the wall by increasing the number/diameter of the installed anchors or by improving the mechanical characteristic of the wall with local interventions (injections, deep-repointing etc.). These types of intervention would determine a higher initial stiffness and strength of the wall, reducing the inward shift $u_\theta(\vartheta)$, so that the block's behaviour would approach the response of a block on a rigid surface. According to various authors who investigated the beneficial effects of injections and deep repointing intervention on the stiffness of wall panels [26[27], an increase up to 20% of the initial stiffness can be achieved. It is found that an increment of 20% of the initial stiffness by injection/repointing and an increment in the diameter of the anchors by 30% would provide enough strength to resist the considered seismic action. Point PP in Fig. 4b shows that the seismic demand will require the anchor to be fully in its plastic phase, with considerable permanent deformations equal to Δ_upl = 64 mm for the considered case. These types of interventions need to be weighed up on a case-by-case basis, depending on the state of the building before the intervention. For the case of monumental buildings, the principles of minimum intervention and non-intrusiveness enshrined in the ICOMOS/ISCARSAH chart [28] regulate the feasibility of the intervention.
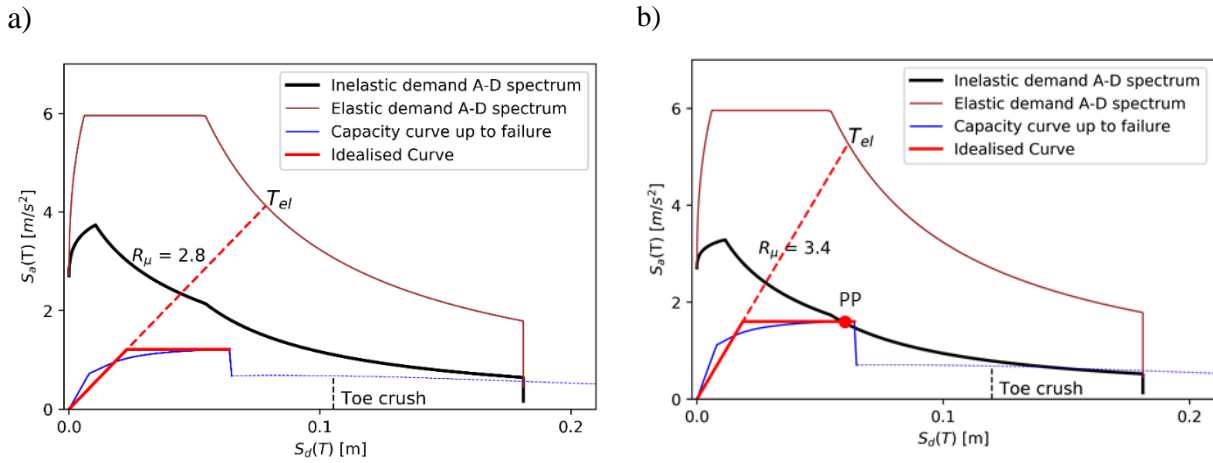
a)

b)

Fig. 4. Performance point determination for a restrained wall a) before strengthening intervention b) after strengthening intervention (injection/repointing and increase of bar's diameter).

4. Dissipative anchoring system

A less intrusive way of improving the seismic response of the restrained wall would be by increasing the ductility capacity of the system (μ). As previously stated, the system's failure is reached for the ultimate elongation of the steel bar $S_{d_{pl}}$, which is proportional to the ultimate strain ϵ_{pl} and the length of the bar. Increasing μ would require an increase of the bar's length (which is constrained by the geometry of the problem), or the choice of a material with proportionally longer plastic deformation. Alternatively, the application of dissipative devices as additional element to steel ties offers a contribution in this sense. The use of Shape Memory Alloys Devices (SMADs) was proposed by [29] in connection with horizontal or vertical steel ties to behave plastically under high-intensity horizontal actions. Owing to their particular stress-strain relationship, the SMADs can allow for "controlled displacements" of the anchorage, lessening the stiffness of the connection and thus preventing the typical failure of traditional steel-ties anchorages. More recently, D'Ayala and Paganoni, have developed a dissipative anchoring system that could combine the availability of anchorages and the energy dissipation capacity of a friction-base device [12]. Once inserted at the connection between perpendicular walls (Fig. 5b), the stainless steel profiles improve the box-like behaviour of the building, while the device allows for a controlled displacement of the walls. For this study, the design of a wall restrained with the dissipative anchoring system is proposed and compared with the design cases previously discussed to assess the benefit of introducing such an innovative device.

a)

b)

Fig. 5. Friction-based Dissipative device proposed by D'Ayala and Paganoni, b) insertion of dissipative anchoring system at the connection between orthogonal walls.

8

4.1 Design of dissipative anchoring system

The design of a friction-based device is based on the Coulomb equation of friction:

$$F_{\text{fric}} = n \, \beta \, F_{\perp} \tag{16}$$

Which states that the maximum friction force (F_{fric}) generated by the slippage of elements in contact is dependent on the applied perpendicular force ($F_{\perp}$), the friction coefficient, β, and the number of surfaces in contact, n. Any force smaller than F_{fric} is not able to cause the relative motion between the elements. Regarding the dissipative device proposed by D'Ayala and Paganoni, shown in Fig. 5a, the friction force is generated by compressing the pair of outer plates around the sliding element. The device has a set of bolts passing through the assembly that can be tightened to achieve the desired perpendicular force and a central pin that regulates the allowable run of the internal slider to a maximum of 3 cm. When connected to the steel bar, the dissipative anchoring system is tuned to start sliding for a force (F_{sliding}) smaller than the yielding force of the bar (F_{yield}). Once the maximum allowable run is achieved ($\Delta u_{dev} = 3$ cm) the system behaves like a normal anchor up to ultimate failure, as shown in Fig 6b. With reference to Fig. 6a, the equilibrium equation also considering the contribution of the dissipative anchoring system is:

$$mg \, \text{R}\sin(\alpha - \vartheta) - mg \, u_\theta(\vartheta) + F_{dev}(\vartheta)H_t = \lambda \, mgR \cos(\alpha - \vartheta) \tag{17}$$

Where:

$$F_{dev}(\theta) = \begin{cases} \dfrac{H_t \tan(\vartheta)}{L_t} EA & 0 < \theta \leq \theta_{dev1} \\ \epsilon_{dev1} EA & \theta_{dev1} < \theta \leq \theta_{dev2} \\ \dfrac{H_t \tan(\vartheta)}{L_t} EA & \theta_{dev2} < \theta \leq \theta_y \\ \epsilon_y EA & \theta_y < \theta \leq \theta_{pl} \\ 0 & \theta \geq \theta_{pl} \end{cases} \tag{18}$$

F_{dev} is the force provided by the dissipative anchoring system, H_t , L_t is the vertical distance between A and O and length of anchoring system. With reference to Fig. 6a, the rotation identifying the beginning and end of the sliding motion are $\theta_{dev1} = arctan(\epsilon_{dev1} \, L_t/H_t)$ and $\theta_{dev2} = arctan(\epsilon_{dev2} \, L_t/H_t)$, while the rotations corresponding to the yielding of the anchor (θ_y) and its maximum plastic deformation (θ_{pl}) are:

$$\theta_y = arctan(\left(\frac{\Delta u_{dev}}{L_t} + \epsilon_y\right) L_t/H_t)$$

$$\theta_{pl} = arctan(\left(\frac{\Delta u_{dev}}{L_t} + \epsilon_{pl}\right) L_t/H_t) \tag{19}$$

The design of the restrained wall follows the same procedure described in the previous section. The system's capacity curve is shown in Fig. 7a, along with the idealized linear-plastic approximation. Whit reference to the idealized curve, the ductility capacity of the system is computed as:

$$\mu_{capacity} = \frac{\Delta_u}{\Delta_y} = \frac{1}{2\left(1 - \dfrac{E}{S_{a_u}\Delta_u}\right)} \tag{20}$$

9

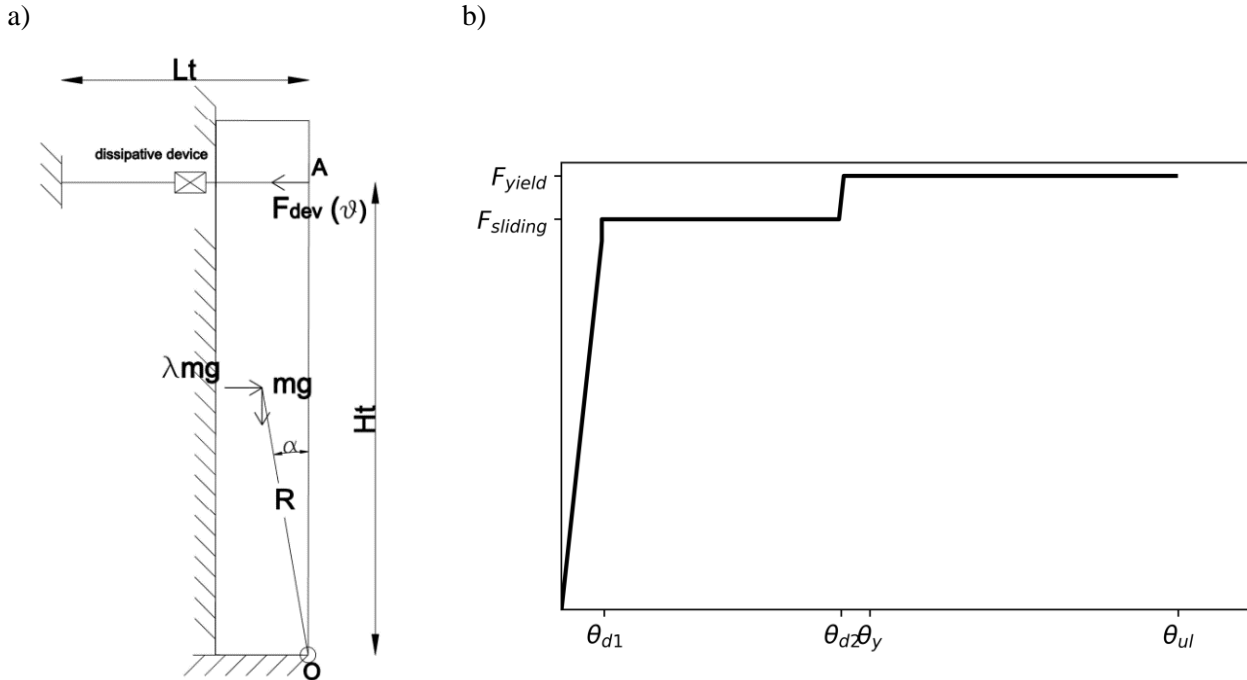a)   b)

Fig. 6. Wall restrained by the dissipative anchoring system: a) Geometrical parameters of one-sided rotation, b) provided resisting force with increasing rotations

The elastic A-D spectrum is then reduced by a reduction factor corresponding to $\mu_{capacity}$ to obtain the inelastic spectrum shown in Fig. 7b. The performance point PP falls on the capacity curve, verifying the system, without exploiting the full plastic deformation capacity of the bar, thus reducing the permanent anchor's deformations. Moreover, the curvature corresponding to the performance point is smaller than the critical curvature (θ_c) that would cause the crushing of compressed corner of the wall at the plastic hinge height.

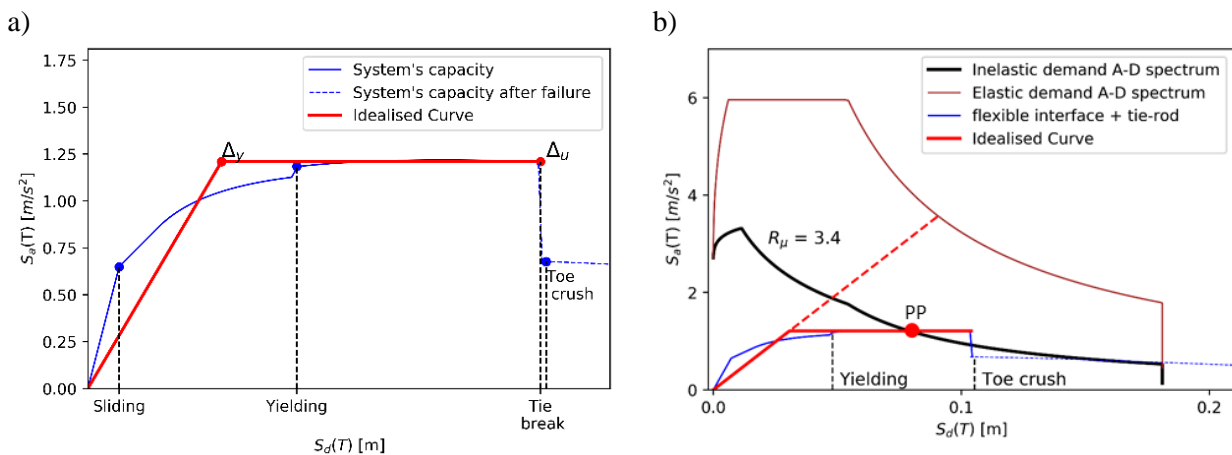a)   b)

Fig. 7. a) capacity curve and idealized capacity curve, b) Design check for wall strengthened by a dissipative anchoring system.

5. Conclusions

In this article, the results of nonlinear pushover analyses of a single-body wall restrained by an elasto-plastic tie rod and an innovative dissipative anchoring system of finite displacement capacity are proposed. Tie rods

10

have been used extensively in the past and are still widely implemented to restore the box-like behaviour between resisting walls and redistribute the seismic forces. The innovative system is designed to be connected in series with the tie rods to provide additional ductility and energy dissipation capacity. The response has two sources of nonlinearity, one geometry-related and one material-related. The model takes into account the ductility capacity of the two systems: the tie's ductility depends on the difference between the ultimate and the yield deformation, while the dissipative system provides an additional contribution given by the maximum allowable run of the slider. The design of the different systems is proposed for a predetermined seismic action, according to a displacement-based approach. Within the framework of the N2 method, the capacity curves of the two systems are compared with the seismic demand to identify a performance point representative of the structure's performance. In both cases, the systems' ultimate capacity corresponds to the ultimate deformation of the tie, which is the first element to fail. The results show that the initial dimensions of the tie are not sufficient to provide the required displacement demand, as the performance point would fall outside the capacity curve. Increasing the diameter of the anchor by 30% and the initial stiffness of the wall by 20% performing injection/repointing interventions would provide enough strength to resist the considered seismic action. Conversely, the introduction of the dissipative device increases the controlled displacement capacity of the restrained wall by 62% and increases the ductility by 21%, allowing for a further demand's reduction. The analysis's results show that the required seismic displacement demand is obtained by the full exploitation of the device's sliding capacity and partially by the plastic yielding of the tie, which permanently deforms for 30% of the its ultimate deformation. It can be concluded that the design drift for a life-safety performance is obtained since the displacement demand is smaller than the displacement ($S_{\theta c}$) that would cause the crushing of the compressed toe at the plastic hinge's location. These results highlight that the dissipative device is fit for the seismic strengthening of masonry structures. In particular, historic buildings would benefit of the implementation of the innovative system because it would reduce the size of the required tie-rods, resulting in less invasive installation procedures.

6. References

[1] D'Ayala, Dina F. and Sara Paganoni. 2011. "Assessment and Analysis of Damage in L'Aquila Historic City Centre after 6th April 2009." Bulletin of Earthquake Engineering 9(1):81–104.

[2] Moon, Lisa, Dmytro Dizhur, Ilaria Senaldi, Hossein Derakhshan, and M. C. Griffith. 2014. "The Demise of the URM Building Stock in Christchurch during the 2010 – 2011 Canterbury Earthquake Sequence." (January 2015).

[3] Putrino, Valentina and Dina D'Ayala. 2018. "Cumulative Damage Assessment and Strengthening Efficacy of Masonry Building in Norcia Affected by the 2016 Seismic Events in Central Italy - For the 2017 EEFIT Research Award."

[4] Doglioni, F., Moretti, A. & Petrini, V. 1994. Le chiese e il terremoto. Trieste: Edizioni LINT (in Italian).

[5] D'Ayala, D. and E. Speranza. 2003. "Definition of Collapse Mechanisms and Seismic Vulnerability of Historic Masonry Buildings." Earthquake Spectra 19(3):479–509.

[6] Lagomarsino, S. and S. Resemini. 2005. "Mechanical Models for the Seismic Vulnerability Assessment of Churches." 1091–1102.

[7] Paganoni, Sara and Dina D'Ayala. 2014. "Testing and Design Procedure for Corner Connections of Masonry Heritage Buildings Strengthened by Metallic Grouted Anchors." Engineering Structures 70:278–93.

[8] CMIT 2009. Circolare Del Ministro Delle Infrastrutture e Dei Trasporti 2 Febbraio 2009, n. 617, Contenente Le Istruzioni per l′applicazione Delle ″Nuove Norme Tecniche per Le Costruzioni″ Di Cui Al DM 14 Gennaio 2008. Gazzetta Ufficiale n. 47 del 26 Feb 2009.

[9] Giovinazzi, S., S. Lagomarsino, and S. Resemini. 2006. "Displacement Capacity of Ancient Structures through Non-Linear Kinematic and Dynamic Analyses." 1–10.

[10] Freeman, Sigmund A. 2004. "Review of the Development of the Capacity Spectrum Method." 41(438):1–13

[11] 1998:2005, EN. 2011a. "Eurocode 8: Design of Structures for Earthquake Resistance. Part 1 : General Rules, Seismic Actions and Rules for Buildings." 1(2004).

[12] D'Ayala, D. F. and S. Paganoni. 2014. "Testing and Design Protocol of Dissipative Devices for Out-of-Plane Damage." Proceedings of the Institution of Civil Engineers: Structures and Buildings 167(1).

[13] James, P., Lee J., S. Paganoni, and D'Ayala D. 2014. "Building Anchoring System."

[14] Melatti, Victor and Dina D'Ayala. 2018. "Dissipative Device for the Seismic Protection of Masonry Structures." 16th European Conference on Earthquake Engineering 1–12.

[15] Melatti, V., D'Ayala, D., Modolo, E., Computational Validation of Dissipative device for the Seismic Upgrade of Historic Buildings, Computational Methods in Structural Dynamics and Earthquake Engineering, 2019.

[16] OPCM, no. 3431, 3 May 2005. Official Bullettin no. 107, 10 May 2005 (in Italian)

[17] D'Ayala, D. 2013. Assessing the Seismic Vulnerability of Masonry Buildings, In Handbook of   Seismic Risk Analysis and Management of Civil Infrastructure Systems; Tesfamariam, S., Goda, K.,   Eds.; Woodhead Publishing: Cambridge, UK, 2013; pp. 334–365

[18] Lagomarsino, Sergio. 2015. "Seismic Assessment of Rocking Masonry Structures." 97–128.

[19] Costa, Alexandre A., Arêde, A., Penna, A., Costa, Aníbal, Free rocking response of a regular stone masonry wall with equivalent block approach: experimental and analytical evaluation, Earthquake engineering and structural dynamics, 2013, pp 2297-2319.

[20] Mehrotra, A., and M. J. DeJong. 2018. The influence of interface geometry, stiffness, and crushing on the dynamic response of masonry collapse mechanisms. Earthquake Engineering & Structural Dynamics 47(13):2661–81. Wiley-Blackwell. doi:10.1002/eqe.3103

[21] AlShawa, o., Liberatore L., Liberatore D., F. Mollaioli, and L. Sorrentino. 2019. "Seismic Demand on a Unreinforced Masonry Wall Restrained by Elasto-Plastic Anchors Under Earthquake Sequences." International Journal of Architectural Heritage 3058, 2019

[22] Magenes, G., A. Penna, I. Senaldi, M. Rota, and A. Galasco. Shaking table test of a strengthened full-scale stone masonry building with flexible diaphragms. International Journal of Architectural Heritage 8 (3):349–75. 2014

[23] Fajfar, P., Gaspersic, P., The N2 method for the seismic damage analysis of RC buildings, International association for earthquake engineering, 1996

[24] FEMA-356 Prestandard and Commentary for the Seismic Rehabilitation of Buildings, Federal Emergency Management Agency (FEMA) Doc. No 356

[25] EN 1993-1-1 (2005) (English): Eurocode 3: Design of steel structures - Part 1-1: General rules and rules for buildings [Authority: The European Union Per Regulation 305/2011. 2005

[26] Perret , S., Khayat K., Gagnon, E., Repair of 130-Year Old Masonry Bridge using High-Performance Cement Grout. Journal of Bridge Engineering. 2002

[27] Corradi, M. 2008. "Experimental Evaluation of Shear and Compression Strength of Masonry Wall before and after Reinforcement : Deep Repointing." 2008.

[28] ICOMOS. 2003. "Principles for the Analysis, Conservation and Structural Restoration of Architectural Heritage (2003)." Architectural Heritage 3–6.

[29] Indirli, Maurizio and Maria Gabriella Castellano. 2008. "Shape Memory Alloy Devices for the Structural Improvement of Masonry Heritage Structures." International Journal of Architectural Heritage 2(2):93–119.